Fermi National Accelerator Laboratory

FERMILAB-Conf-96/201-E
CDF

Quarkonia Production at CDF

R. Demina
For the CDF Collaboration

Fermi National Accelerator Laboratory
P.O. Box 500, Batavia, Illinois 60510

August 1996

Published Proceedings of the *XIth Topical Workshop on ppbar Collider Physics*,
Padova, Italy, May 27-June 1, 1996

Operated by Universities Research Association Inc. under Contract No. DE-AC02-76CHO3000 with the United States Department of Energy

CDF/ANAL/BOTTOM/CDFR/3747

QUARKONIA PRODUCTION AT CDF
Version IV

R. DEMINA
Fermi National Accelerator Laboratory, Batavia,
IL 60510, USA

for CDF Collaboration

We present the results on J/ψ, ψ', χ_c and $\Upsilon(1S)$, $\Upsilon(2S)$, $\Upsilon(3S)$ production in the proton-antiproton collisions at $\sqrt{s} = 1800\ GeV$ measured with the CDF Detector. Contributions of different production mechanisms are discussed.

1 Introduction

Production of a bound state of heavy quark (c or b) and its antiquark in the proton-antiproton collision provides valuable tests of QCD. The dependance of the production cross section on the transverse momentum (P_t) of the final product helps to understand the underlining mechanisms of the production. The relatively high leptonic branching ratios of J/ψ, ψ' and Υ make them the primary objects to study in the high background environment of the high energy proton-antiproton collisions.

2 Quarkonia Production Mechanisms in $p\bar{p}$ Collisions

Several mechanisms are responsible for the charmonia production in the high energy proton-antiproton collisions. At high P_t to $O(\alpha_s^3)$ a $c\bar{c}$ system can be produced in its $^1S_0$ and ^3P_J state [1], which are called η_c and χ_{cJ} respectively. J/ψ can be produced as a result of the radiative decay of χ_{c1} and χ_{c2}: $\chi_c \rightarrow J/\psi + \gamma$. Direct production of the $^3S_1$ state is suppressed. χ_c decay does not contribute to the ψ' production, because it has higher mass. Other possibility to produce charmonium is via B-decay [1]. The overall rate of J/ψ production at $\sqrt{s} = 630 GeV$ was reasonably well described by the above mechanisms [2], but the 88-89 CDF data at $\sqrt{s} = 1800 GeV$ showed a significant excess in both J/ψ and ψ' production [3]. To explain this discrepancy new production mechanisms were introduced, which involve parton fragmentation into ^3P_J states [4]. Though higher order in α_s than direct production, gluon fragmentation may dominate at high P_t. Matrix element for these processes were normalized using $B \rightarrow \chi$ decay rates measured by CLEO [5]. Introduction of the gluon fragmentation into ^3P_J states brought theory to a factor of 3-5 discrepancy with the J/ψ

a). b).

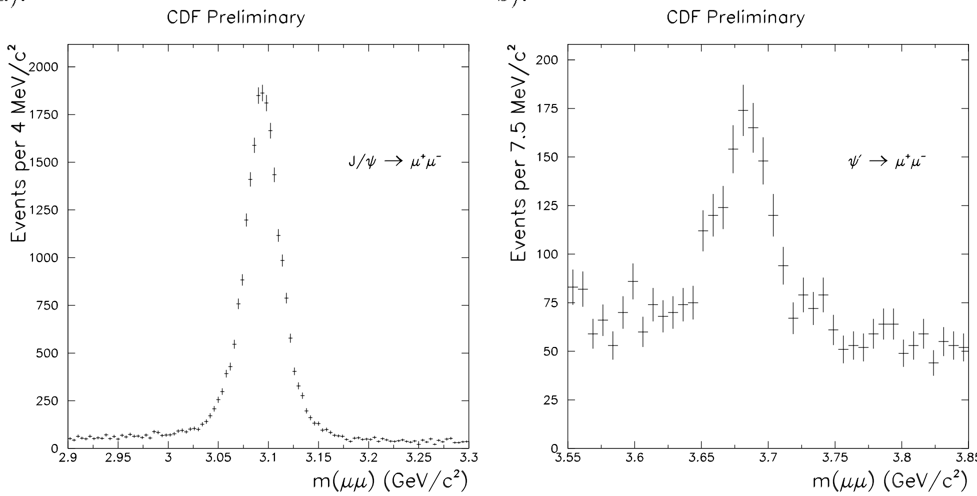

Figure 1: The dimuon invariant mass in the J/ψ(a) and ψ'(b) mass region.

data, but did not explain a factor of 50 discrepancy in the ψ' data. Later the possibility of the decay of the states above $D\bar{D}$ threshold into ψ' were discussed[6]. Other way to produce J/ψ and ψ' is via gluon fragmentation into color octet $^3S_1$ state[7]. Since these diagrams involve emission of an extra gluon they are suppressed by a factor of $\alpha_s v^2$, where v- is the relative velocity of the quarks, with respect to gluon fragmentation into ^3P_J states, but could be important for ψ' production and may explain the excess in the J/ψ data. Since these diagrams involve long scale processes like soft gluon emission, their matrix elements are difficult to calculate analytically. The absolute values of these matrix elements were used as free parameters in the fit to CDF data.

3 The J/ψ and ψ' Production

The J/ψ and ψ' are detected in their decay into a muon pair:

$$p\bar{p} \rightarrow J/\psi(\psi') \; + \; X, \; J/\psi(\psi') \rightarrow \mu^+\mu^- .$$

The total luminosity accumulated in 92-93 Tevatron run is about 20 pb^{-1}. Two muons with minimum $P_t > 2.2 \; GeV/c$, maximum $P_t > 2.8 \; GeV/c$ and the invariant system $P_t > 5 \; GeV/c$ in the $|\eta| < 0.6$ region have been selected. The invariant mass distribution of the dimuon system is shown in figure 1,

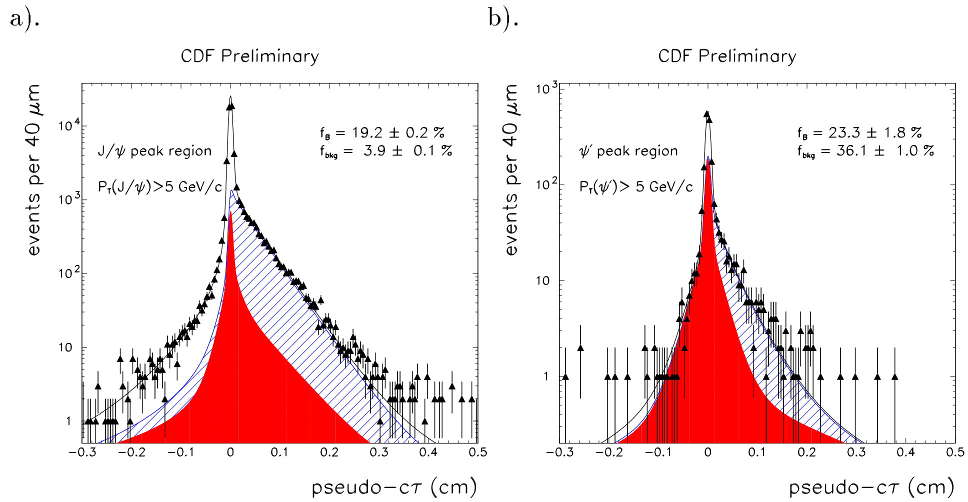

Figure 2: The J/ψ(a) and ψ'(b) $c\tau$ distribution, solid line is a result of the fit, dark region is the background contribution, shaded region - B-component, prompt is the rest.

for the J/ψ an ψ' mass regions. The corresponding total cross section times branching ratios are:

$$\sigma(\bar{p}p \rightarrow J/\psi)Br(J/\psi \rightarrow \mu^+\mu^-) = 17.35 \pm 0.14(stat) \pm^{2.59}_{2.79} (sys)\ nb,$$

$$\sigma(\bar{p}p \rightarrow \psi')Br(\psi' \rightarrow \mu^+\mu^-) = 0.571 \pm 0.036(stat) \pm^{0.082}_{0.089} (sys)\ nb.$$

The significant accumulated statistics and the precision of the silicon vertex detector allow not only to study the P_t dependance of the production rate, but to separate different production mechanisms, like B and χ-decays.

3.1 The J/ψ and ψ' B-fractions

The information from the Silicon VerteX detector(SVX) is used to separated prompt and B-decay production components. First two muon tracks are used to determine the two-dimensional decay length (L_{xy}). To determine the proper lifetime ($c\tau$) one must divide the L_{xy} by $\beta\gamma$ factor of the parent B-meson. Monte Carlo is used to correct for the unobserved particles in B-decay: $(\beta\gamma)_{J/\psi} \rightarrow (\beta\gamma)_B$. The $c\tau$ distributions for J/ψ and ψ' (Figure 2) were fitted to three components: prompt, B-decay and background. The shape of the prompt component is a gaussian, B-decay - is a b-lifetime distribution convoluted with the resolution function, the background shape has been determined

a). b).

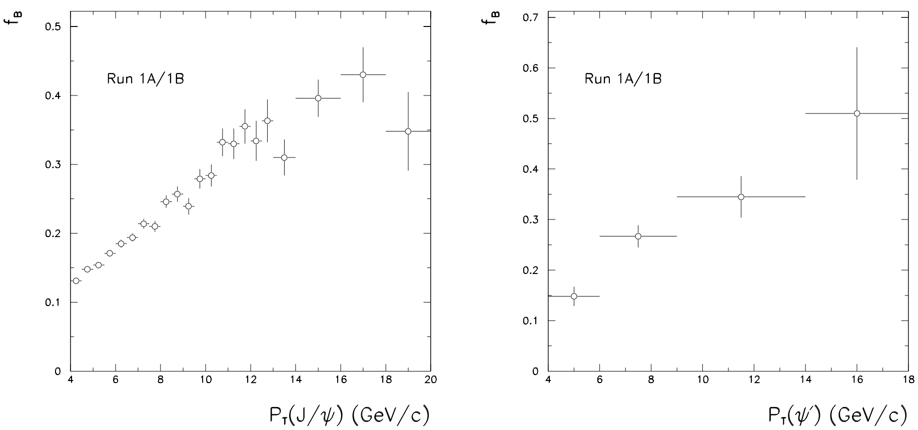

Figure 3: The P_t dependance of the B-fractions for J/ψ(a) and ψ'(b).

from the side bands and is a gaussian with positive and negative exponential tails. The determined J/ψ and ψ' B-fractions are:

$$F_B^{J/\psi}(P_t > 5\ GeV/c) = 19.2 \pm 0.2(stat) \pm 0.4(sys)\%,$$

$$F_B^{\psi'}(P_t > 5\ GeV/c) = 23.3 \pm 1.8(stat) \pm 0.5(sys)\%.$$

The P_t dependance of the B-fractions are shown in figure 3 and the corresponding J/ψ and ψ' B-cross sections are presented in figure 4. The theory curves are NLO QCD B-production with MRSD0 structure functions. This measurement is consistent with the other B-cross section measurements done by CDF[8].

3.2 χ_c Fraction

Both LO and parton fragmentation mechanisms involve J/ψ production via χ_c decay. To separate these mechanisms a photon from $\chi_c \rightarrow J/\psi + \gamma$ decay is reconstructed. The photon energy threshold is 1 GeV. Electromagnetic calorimeter energy resolution $\frac{\Delta E}{E} = \frac{14\%}{\sqrt{E}}$ is not enough to resolve separate χ_c states. The fraction of J/ψ coming from χ_c decay has been determined to be :

$$F_{\chi}^{J/\psi} = 28.3 \pm 1.6(stat) \pm 6.8(sys)\%.$$

a). b).

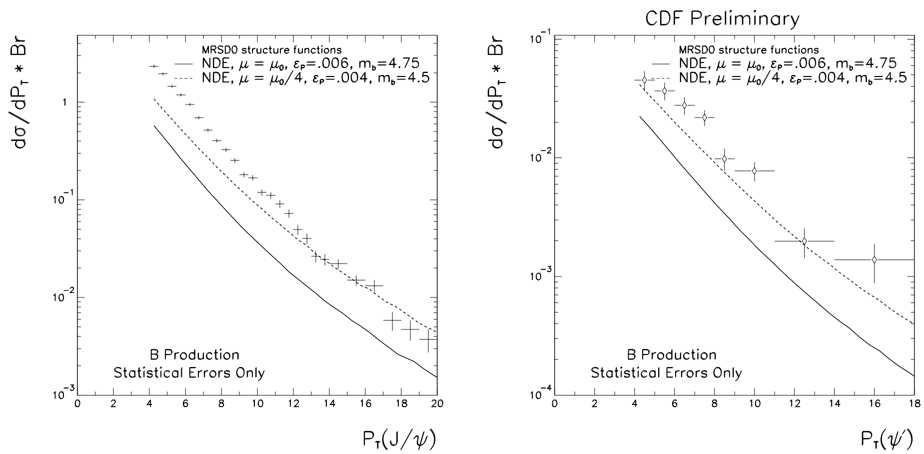

Figure 4: J/ψ(a) and ψ'(b) differential cross sections from B-decay. The theory curves are NLO QCD B-production with MRSD0 structure functions.

The branching ratio of $B \rightarrow \chi_c$ measured by CLEO [5] has been used to exclude the B-contribution to χ_c fraction:

$$F(No\, B)_{\chi}^{J/\psi} = 32.3 \pm 2.0(stat) \pm 8.5(sys)\%.$$

The corresponding cross section is shown in figure 5. The theory curve has been provided by M.Mangano [9] and includes both LO and parton fragmentation production mechanisms.

3.3 Prompt J/ψ and ψ' production

B and χ_c decay contributions have been subtracted from the total cross section (figure 6). There is a significant discrepancy between the data points and the singlet production predictions. As it has already been mentioned the gluon fragmentation matrix elements are parameters in the fit to the data. The P_t dependance of the prompt production cross sections of the J/ψ and ψ' production is described well by the gluon fragmentation.

4 Υ Production

$\Upsilon(1S)$, $\Upsilon(2S)$, $\Upsilon(3S)$ represent another heavy quark-antiquark system. Similarly to ψ it was studied in its decay to two muons: $p\bar{p} \rightarrow \Upsilon + X$, $\Upsilon \rightarrow \mu^+\mu^-$.

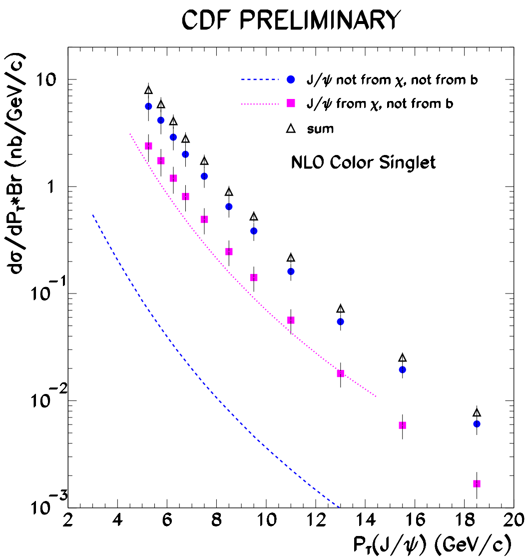

Figure 5: χ_c and non-χc components of the J/ψ cross section. The theory curve includes both LO and gluon fragmentation production mechanisms.

a). b).

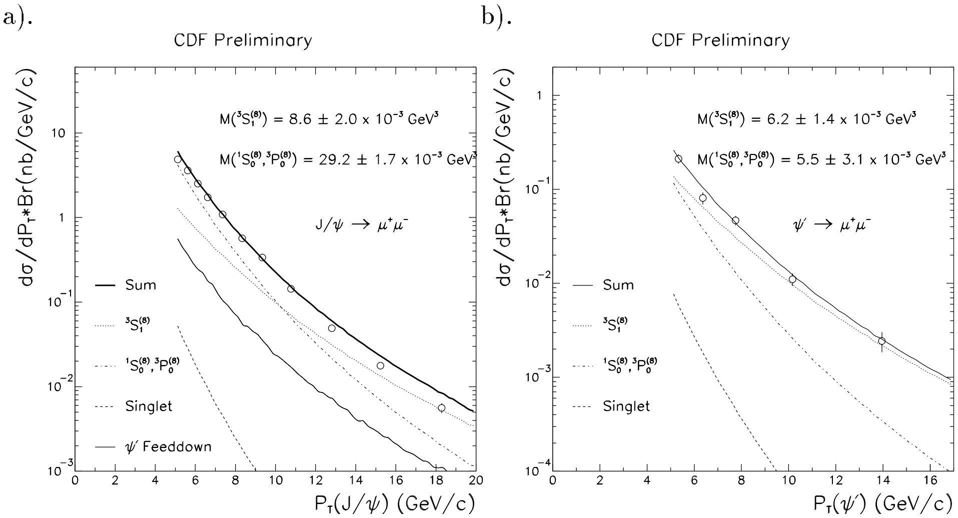

Figure 6: The J/ψ(a) and ψ'(b) prompt cross sections, B and χ_c contributions subtracted. Solid curves are results of fitting the gluon fragmentation shapes to the data points.

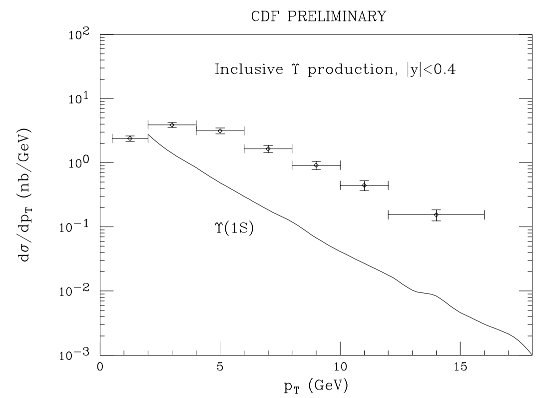

Figure 7: Production cross section for $\Upsilon(1S)$. Solid curve shows the LO QCD predictions.

The CDF analysis based on 16 pb^{-1} data has been published in ref. [10]. Two muons with minimum $P_t > 2.2 GeV/c$ and maximum $P_t > 2.8 GeV/c$ have been selected in the pseudorapidity region $|\eta| < 0.4$. The total production cross sections of $\Upsilon(1S)(2S)(3S)$ production times the branching ratio are:

$$\frac{d\sigma}{dy}(\bar{p}p \to \Upsilon(1S),\ y=0,\ 0 < P_t < 16\ GeV/c) * Br(\Upsilon(1S) \to \mu^+\mu^-) =$$

$$= 753 \pm 29(stat) \pm 72(sys)\ pb;$$

$$\frac{d\sigma}{dy}(\bar{p}p \to \Upsilon(2S),\ y=0,\ 1 < P_t < 10\ GeV/c) * Br(\Upsilon(2S) \to \mu^+\mu^-) =$$

$$= 183 \pm 18(stat) \pm 24(sys)\ pb;$$

$$\frac{d\sigma}{dy}(\bar{p}p \to \Upsilon(3S),\ y=0,\ 1 < P_t < 10\ GeV/c) * Br(\Upsilon(3S) \to \mu^+\mu^-) =$$

$$= 101 \pm 15(stat) \pm 13(sys)\ pb;$$

The P_t dependance of the production cross section is shown in figure 7.

5 Conclusions

The total J/ψ and ψ' cross sections and their P_t dependance have been studied using about 20 pb^{-1} of CDF data. The precision of the SVX detector allowed to use the lifetime information to extract the B-decays component in the J/ψ and ψ' production. B-fraction of the J/ψ and ψ' production was found to increase with P_t. The corresponding b-cross section agrees with the previous CDF measurements.

Fraction of J/ψ from $\chi \to J/\psi + \gamma$ decay was measured and its P_t dependance studied using fully recontructed photons from χ_c decay. The B and χ_c contributions have been subtracted from the total J/ψ and ψ' cross sections, which then were fitted to the sum of LO and parton fragmentation components. The absolute values of the matrix elements of the color-octet fragmentation diagrams were free parameters in the fit, but the P_t behavior of the data was reproduced well. This may indicate that the excess in the prompt J/ψ and ψ' production may be explained by the parton fragmentation. Since color-octet fragmentation mechanism predicts certain polarization of the quarkonia states this analysis is in progress on CDF.

6 Acknowledgements

We thank the Fermilab staff and the technical staffs of the participating institutions for their vital contributions. This work was supported by the U.S. Department of Energy and National Science Foundation; the Italian Istituto Nazionale di Fisica Nucleare; the Ministry of Education, Science and Culture of Japan; the Natural Sciences and Engineering Research Council of Canada; the National Science Council of the Republic of China and the A. P. Sloan Foundation.

References

1. R. Baier & R. Ruckle, *Z. Phys.* C **19**, 251 (1983). E. Glover et al., *Z. Phys.* C **38**, 473 (1988).
2. Albajar et al., The UA1 Collaboration, *Phys. Lett.* B **213**, 405 (1988) Albajar et al., The UA1 Collaboration, *Phys. Lett.* B **256**, 121 (1991)
3. F. Abe et al., The CDF Collaboration, *Phys. Rev. Lett.* **69**, 3704 (1992)
4. E. Braaten, M.A. Doncheski, S. Fleming and M.L. Mangano, *Phys. Lett.* B **333**, 548 (1994); M. Cacciari and M. Greco, *Phys. Rev. Lett.* **73**, 1586 (1994); D.P. Roy and K. Sridhar, *Phys. Lett.* B **339**, 141 (1994).
5. CLEO Collaboration Report No. CLEO CONF 94-11.
6. F. Close *Phys. Lett.* B **342**, 369 (1995).
7. M. Cacciari, M. Greco, M.L. Mangano and A. Petrelli, *Phys. Lett.* B **356**, 553 (1995); P. Cho and A.K. Leibovich, Phys.Rev.D53 (1996)150, 6203; E. Braaten & S. Fleming *Phys. Rev. Lett.* **74**, 3347 (1995); P.Cho & M.Wise *Phys. Lett.* B **346**, 129 (1995).
8. F. Abe et al., The CDF Collaboration, *Phys. Rev. Lett.* **75**, 1451 (1995)

9. M. Mangano, private communication.
10. F. Abe et al., The CDF Collaboration, ***Phys. Rev. Lett.*** **75**, 4358 (1995)